Non-Linear Modeling of the Kink Effect in Deep Sub-micron SOI MOSFET

Alexandre Siligaris, Gilles Dambrine, François Danneville

: IEMN CNRS UMR 8520, Avenue Poincaré, BP 69, 59652 Villeneuve d'ASCQ, France
e-mail: alexandre.siligaris@iemn.univ-lille1.fr

tel: +33 (0)3 20 19 79 79, fax: +33 (0)3 20 79 78 92

***Abstract* — Starting from an empirical non-linear model developed for deep sub-micron channel MOSFETs, we present a new model for floating body SOI MOSFETs. It introduces a new non-linear current model for the kink effect, which takes into account of the related frequency dispersion. The model reproduces very well the AC experimental properties related to the kink effect in floating body devices. As an application, it is used in the framework of large signal simulations to study the impact of the kink effect on the third order intermodulation point.**

***Index Terms* — Non linear RF modeling, MOS SOI transistors, low frequency effects, kink effect, intermodulation.**

I. INTRODUCTION

MOSFET devices on SOI substrate show very good microwave performances and it is the most promising technology whenever low cost, low voltage supply and low power consumption are required [1]. The SOI MOS is generally classified in two categories depending on the thickness of the active Silicon layer above the Buried Oxide. The first category is the thin film transistors which are Fully Depleted (FD); the other is the thick film transistors which are Partially Depleted (PD) [2]. One of the resulting electrical differences between the two types is the well known Kink effect on the DC drain current characteristics for the PD nMOSFET's.

Many studies have been carried out on this effect and its impact on the high frequency performances of the devices: f_t, f_{max}, NF_{min}, g_d, low frequency noise, phase noise in oscillators and linearity [2-8]. The kink effect is directly related to the floating body potential in PD devices; it is a low frequency mechanism which disappears over the MHz frequency range. It is responsible for a low frequency noise overshoot that is upconverted into phase noise in feedback oscillators [3, 4]. This effect also degrades the linearity of the floating body devices when the operating frequency is very low [5]. For higher frequency of operation, a theoretical discussion is proposed in [6], showing that the OIP3 of a device may be affected by the kink effect whenever two signals owe frequency shift ($\Delta\omega$) in the same frequency range for which occurs the kink effect. On the other hand, the harmonic distortion is not influenced by the kink in high frequency operation regime [7]. Note that at the process level, the kink can be completely suppressed by using body ties, but this solution is still a point of discussion, because of additional parasitic capacitance which degrades the high frequency performance [5, 8].

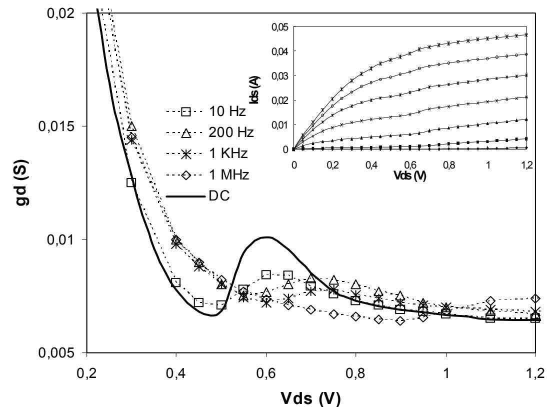

Fig. 1. Measured output drain conductance g_d versus the drain to source DC bias V_{ds} for various frequencies, of a PD floating body MOS with Lg=0.12 µm. V_{gso}=0.6 V. The conductance measurements where made with a HP-4192A LCR meter. The inset shows the measured static drain to source current of the device.

In this paper, the validity of an empirical non linear model developed for kink free MOSFET device [9] (bulk or SOI type) is extended to floating body SOI MOSFETs. This extension is carried out through the addition of close form analytical expressions which describe accurately the Kink effect (and its associated frequency dispersion) occurring in those devices. In addition to modeling accurately the DC and AC properties of PD SOI devices, the model can be used in non linear circuit simulator to study the large signal properties of mixers and oscillators down to the millimeter wave range. As application of the model, OIP3 determination as a function of the load is investigated and a comparison with kink free SOI device is undertaken.

II. KINK EFFECT IN SOI PD nMOSFET

Impact ionization due to high electrical field near the drain, generates hole and electron pairs. The electrons move rapidly to the drain region and the holes move towards the floating body region where the potential is lower. There, their accumulation gives a rise to the body potential V_{bs} and as a consequence, the diode between the body and the source is forward biased and a kink current occurs. The kink effect is observable on the DC drain current characteristics of nMOS PD FB transistors and on their output conductance g_d, as shown on figure 1. The effect is frequency dependent and it disappears for high frequencies because of AC body potential V_{bs} filtering through the junction capacitance C_{bs} between the body and the source [2, 5].

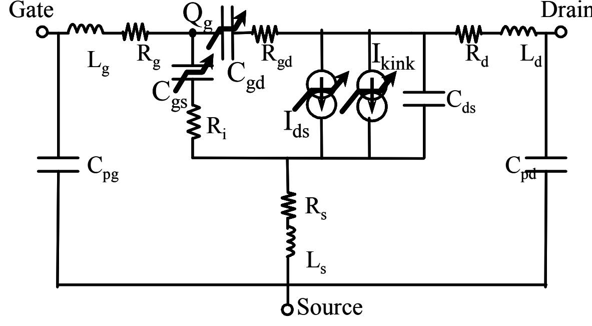

Fig. 2. Non linear model for the SOI MOS. The non-linear elements are denoted by an arrow.

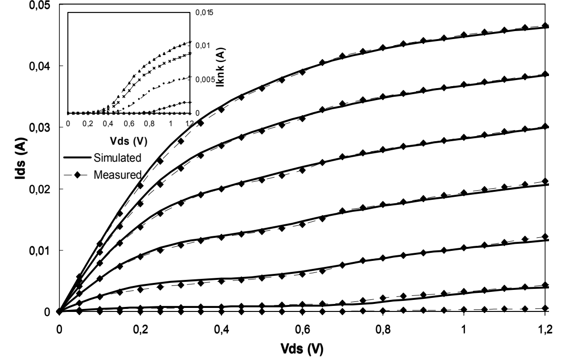

Fig. 3. Static drain current versus V_{ds} for different values of V_{gs}. Symbols correspond to the measurements and the solid line to the simulation. The inset shows the simulated static kink current versus drain bias for various gate biases (V_{gs} *: 0* to *1.2 V*).

III. SOI MOSFET MODEL

The component studied and used for modeling is a PD floating body technology of ST microelectronics, with a gate length of $L_g=0.12$ µm and a total gate width of $n_f x W_f=60x1$ µm. The SOI MOS model is presented on figure 2 and it is very close to the one developed in [9]. It takes into account the non linear drain to source current I_{ds} and the non linear gate to source and gate to drain capacitance C_{gs} and C_{gd} respectively. The capacitance model used here is the same that in [9].

The non linear drain current equation is divided in two components: a DC drain current I_{ds} whose equation is the same as in [9], and a new kink current equation I_{kink}. The total current I_{dsT} is given by:

$$I_{dsT} = I_{ds} + I_{kink} \tag{1}$$

with:

$$I_{ds} = I_{pk}\left[1 + P(V_{gs})tanh(\Psi)\right]\left[P(V_{gd})tanh(V_{ds}(\alpha + K_7 V_{gs}))\right] \tag{2}$$

$$I_{kink} = I_{ks} V_{gs} V_{ds}\left(1 + cV_{ds}\right)\left[1 + tanh\left(a\left(V_{ds} - \frac{b}{V_{gs} + V_{th}}\right)\right)\right] \tag{3}$$

V_{th} is the measured threshold voltage and the other symbols (I_{ks}, *a, b, c*) are the model's parameters. (3) gives the time domain kink current large signal expression and does not include any frequency term. In order to include a frequency term, (3) has to be expressed in the frequency domain by using the Fourier transform. In a general case where the control voltages $V_{ds}(t)$ and $V_{gs}(t)$ are bounded signals defined for $t \in \Re$ it writes :

$$I_{kink}(\omega) = \mathcal{F}\{I_{kink}(t)\} = \int_{-\infty}^{+\infty} e^{-j\omega t} I_{kink}(t)dt \tag{4}$$

Next, we introduce in (4) a term modeling the kink effect's frequency distribution :

$$I_{kink}(\omega) = e^{-\omega\tau_k}\int_{-\infty}^{+\infty} e^{-j\omega t} I_{kink}(t)dt \tag{5}$$

In (5), $e^{-\omega\tau_k}$ is the frequency dispersion model; τ_k is time constant related to the kink effect. The role of $e^{-\omega\tau_k}$ is to modulate the amplitude of each Fourier current coefficient at any frequency component (ω). Let us consider the case of a single tone signal of angular frequency ω_0. $I_{kink}(t)$ is periodic, therefore (3) can be expanded in Fourier series; combined with the frequency model it writes :

$$I_{kink}(t) = e^{-\omega\tau_k}\sum_{n=-\infty}^{\infty} I_{kink\,n} e^{jn\omega_0 t} = \sum_{n=-\infty}^{\infty} I_{kink\,n} e^{-|n|\omega_0\tau_k} e^{jn\omega_0 t} \tag{6}$$

In next section simulation results demonstrating this effect are shown. The implementation of a dispersive model in the ADS simulator (*Agilent Technologies*) is formulated using the *Symbolically Defined Devices* (*SDD*). In the *SDD* the large signal current is described by (3) and the frequency dependence by a weighting function defined by $e^{-\omega\tau_k}$.

The drain current parameters are determined via DC drain current measurements and an optimization procedure. First, we extract I_{ds} (2) parameters values by adjusting the equation on the measured current, in the pre-kink region, i.e. for low drain bias, before saturation. The kink's equation parameters (I_{ks}, *a*, *b*, *c*) are determined in the saturation regime for post-kink drain bias, using the same optimization technique. τ_k value is obtained from low frequency measurements of the drain conductance g_d. For that purpose we used a *HP-4192A* precision impedance analyzer. The obtained value is $\tau_k=0.2\ \mu s$.

IV. SIMULATION RESULTS-DISCUSSION

Figure 3 shows the measured and simulated DC drain current I_{dsT}. The symbols are used to illustrate the measurements and the solid line shows the simulated current with the kink component. The inset shows the DC simulated kink current when the I_{ds} (2) is switched off. On figure 4 is illustrated the simulated AC drain conductance g_d versus the drain bias V_{dso} in the inversion regime ($V_{gs}=0.6\ V$) for frequencies from *10 Hz* to *10 MHz*. We see clearly that the kink's frequency dispersion on the g_d is well reproduced by the model. Its cut-off frequency is located around a few *MHz*.

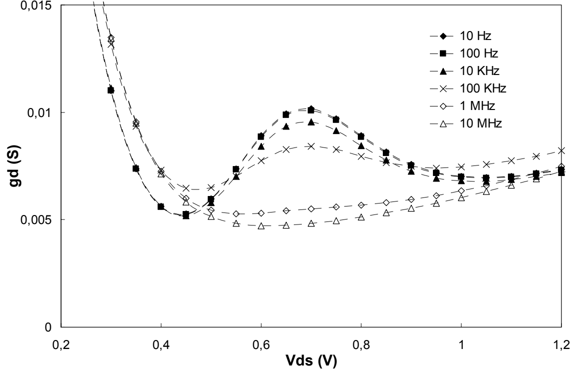

Fig. 4. Simulated AC drain conductance versus the drain bias for frequencies from 10 Hz to 10 MHz.

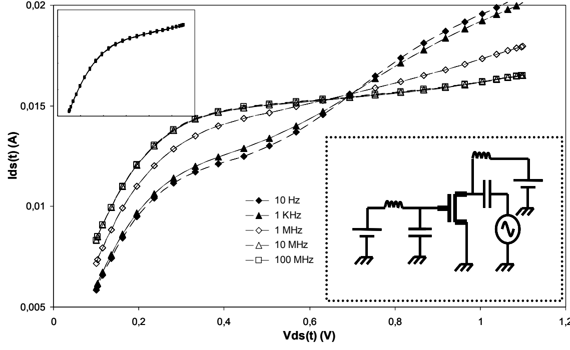

Fig. 5. Simulated instantaneous large signal drain current versus the instantaneous drain voltage (swing =0.5 V) for various frequencies. The up inset shows the same result for a body tied transistor. The down inset shows schematically the simulation bench.

On next figure (fig. 5), is shown the instantaneous large signal current $I_{ds}(t)$ versus the instantaneous drain voltage $V_{ds}(t)$. For that simulation, we applied a large signal on the drain of the device (AC V_{ds} swing: 0.5 V) at various frequencies (*10 Hz* to *100 MHz*) and kept the AC gate voltage shunt to zero. The DC bias is kept at $V_{ds0}=V_{gs0}=0.6\ V$, where the kink effect of this device is at its maximum (fig. 1, 3). At low frequencies, we observe that the large signal current encloses the kink effect, which disappears between *1* and *10 MHz*. The same simulation was performed for a body tied device (up inset of figure 5); in this case we observe that the large signal current of the device is frequency independent.

The validity of equation (6) is shown on figure 6. The inset of the figure gives the first 10 harmonic components of the drain current when the fundamental frequency of the applied large signal (V_{ds} swing : *0.5 V*) is *1 MHz*. The plain symbols are used for the simulated current without (*W/O*) the dispersion term and the bold symbols for the simulated current when the dispersion term is applied (*W*). We notice that there is a difference between the amplitude of the harmonics. The larger the frequency is, the higher this difference is. Figure 6 shows the ratio of the harmonics *W* and *W/O* frequency term, compared to the dispersion model $e^{-\omega\tau_k}$. It is obvious that the simulated result gives exactly the expected theoretical result calculated by (3) and (6) :

$$\begin{array}{c}Theoretical\\ Ratio\end{array} = \frac{I_{kink}(t)\big|_W}{I_{kink}(t)\big|_{W/O}} = \frac{e^{-\omega\tau_k}\sum_{n=-\infty}^{+\infty} I_{kink\,n}\, e^{jn\omega_0 t}}{\sum_{n=-\infty}^{+\infty} I_{kink\,n}\, e^{jn\omega_0 t}} = e^{-\omega\tau_k} \qquad (7)$$

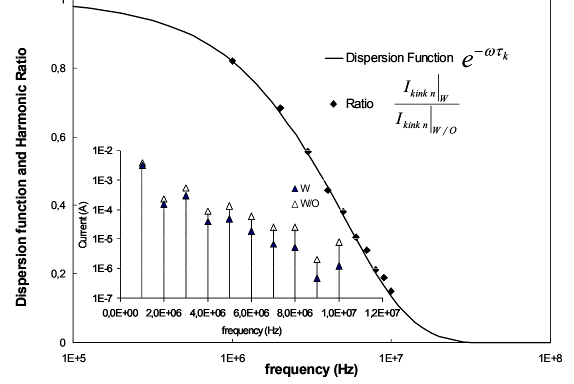

Fig. 6. Inset : Harmonic components of the simulated kink current when a large signal of 1 MHz is applied on the drain (V_{ds} swing =0.5 V). Plain triangles : Without frequency model. Bolt triangles : With frequency model.
Figure : Ratio of the each simulated harmonic (symbols) and frequency model (solid line).

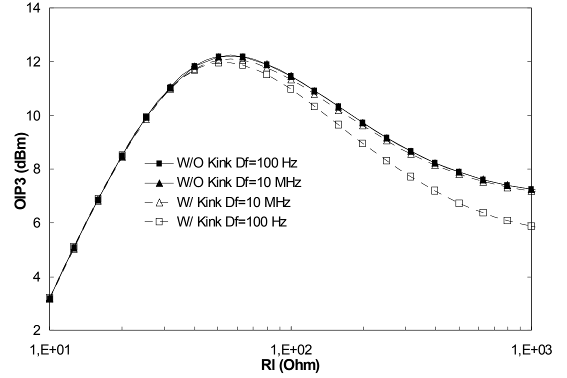

Fig. 7. Simulated OIP3 versus the load resistance with and without kink for two different frequency spacing: Δf=100 Hz and Δf=10 MHz. $V_{dso}=V_{gso}$=0.6 V. f_0=2 GHz. f_1=2 GHz + Δf.

Considering that the model describes correctly the electrical DC as well as AC small signal and large signal characteristics and takes into account the Kink effect and its frequency dispersion, we suggest a discussion on the kink's impact on the device's non-linear properties. For that, we have simulated the third order output intercept point (OIP3) with and without the kink current. The transistor is biased in the kink region ($V_{gso}=V_{dso}=0.6\ V$). We applied a fundamental frequency of 2 GHz and two frequency spacing of *Δf=100 Hz* and *10 MHz*, which are respectively within the kink frequency range and out of the kink cut-off frequency.

Figure 7 shows the OIP3 versus the load resistance R_l for values from *10 Ω* to *1 KΩ*. The solid lines correspond to a simulation for two frequency spacing of *Δf=10 MHz* and *Δf=100 Hz,* in which the kink current I_{ks} is turned off. The dashed lines are used for simulation in which the kink current is turned on and the frequency spacing is *Δf=100 Hz* and *Δf=10 MHz* respectively. We observe that the device show the same OIP3 if the frequency spacing *Δf* is located over the kink frequency cut-off $f_k=1/\tau_k$ whatever might be the load impedance. However, when *Δf* is within the kink frequency domain (*Δf=100 Hz*) and the load impedance is higher than 80 Ω, it comes out that the OIP3 is degraded for the device including kink, even though the operating fundamental frequency is well above the kink's cut-off frequency.

In [10], it has been shown that for MOS bulk devices at high frequency operation (>1 GHz), the 3rd order intermodulation is dominated by the transconductance when the load impedance is low and by the drain conductance when the load impedance is high. Here we show that SOI devices with floating body have the same behavior, moreover that the kink effect degrades the intermodulation at high load impedances if the frequency spacing

Δf is in the kink's frequency domain. This result is also consistent with equations (8-13) in [6] where the low frequency term *gd(Δω)* appears in the OIP3 calculation.

V. CONCLUSION

A new model for the kink effect in PD SOI MOSFETs with floating body is proposed. It takes into account the frequency dispersion of the phenomena. The various small signal and large signal simulations show that frequency effects due to the kink are well reproduced by the model. Finally, we observe that the kink acts as a slow memory effect and degrades slightly in certain conditions the intermodulation of floating body devices compared to body tied ones.

REFERENCES

[1] J.P. Colinge, J.Chen, D.Flandre, J.P.Raskin, R.Gillon and D.Vanhoenacker, "A Low-Voltage, Low-Power Microwave SOI MOSFET," *IEEE International SOI Conference, Proceedings,* pp. 128 - 129, 30 Sept.-3 Oct. 1996

[2] J.P.Colinge, *Silicon-on-Insulator Technology: Materials for VLSI.* 2nd ed. Kluwer Academic Publishers.

[3] Y.-C.Tseng, W.-L.M.Huang, P.J.Welch, J.M.Ford, and J.C.S.Woo, "Empirical Correlation Between AC Kink and Low-Frequency Noise Overshoot in SOI MOSFET's," *IEEE Electron Device Letters*, vol. 19, no. 5, pp. 157-159, May 1998

[4] Y.-C.Tseng, W.M.Huang, E.Spears, D.Spooner, D.Ngo, J.M.Ford, and J.C.S.Woo, "Phase Noise Characteristics Associated with Low-Frequency Noise in Submicron SOI MOSFET Feedback Oscillator for RF IC's," *IEEE Electron Device Letters*, vol. 20, no. 1, pp. 54-56, January 1999

[5] Y.-C.Tseng, W.M.Huang, D.J.Monk, P.Welch, J.M.Ford, and J.C.S.Woo, "AC Floating Body Effects and the Resultant Analog Circuit Issues in Submicron Floating Body and Body-Grounded SOI MOSFET's," *IEEE Transactions On Electron Device*, vol. 46, no. 8, pp. 1685-1692, August 1999

[6] A.O.Adan, T.Yoshimasu, S.Shitara, N.Tanba, and M.Fukumi, "Linearity and Low-Noise Performance of SOI MOSFETs for RF Applications," *IEEE Transactions On Electron Device*, vol. 49, no. 5, pp. 881-888, May 2002

[7] B.Parvais, A.Cerdeira, D.Schreurs, and J.P.Raskin "Harmonic Distortion Characterization of SOI MOSFETs," *European Microwave Week, GaAs Conference, Proceedings,* pp. 357 - 360, September 2003

[8] C.F.Edwards, W.Redman-White, B.M.Tenbroek, M.S.L.Lee, and M.J.Uren, "The Effect of Body Contact Series Resistance on SOI CMOS Amplifier Stages," *IEEE Transactions On Electron Device*, vol. 44, no. 12, pp. 2290-2294, December 1997

[9] A.Siligaris, G.Dambrine, D.Schreurs, and F.Danneville, "A New Empiririical Non-Linear Model for sub-250 nm channel MOSFET," *IEEE Microwave and Wireless Component Letters*, vol. 13, no. 10, pp. 449-451, October 2003

[10] S.Kang, B.Choi, and B.Kim "Linearity Analysis of CMOS for RF Application," *IEEE Trans. Microwave Theory and Techniques,* vol. 51, no. 3, pp. 972-977, March 2003